Bioorganic & Medicinal Chemistry Letters 21 (2011) 3780–3783

Contents lists available at ScienceDirect

Bioorganic & Medicinal Chemistry Letters

journal homepage: www.elsevier.com/locate/bmcl

Novel C8-linked pyrrolobenzodiazepine (PBD)–heterocycle conjugates that recognize DNA sequences containing an inverted CCAAT box

Federico Brucoli [a], Rachel M. Hawkins [a], Colin H. James [a], Geoff Wells [a], Terence C. Jenkins [b], Tom Ellis [c,d], John A. Hartley [c,d], Philip W. Howard [d], David E. Thurston [a,d,*]

[a] The School of Pharmacy, University of London, London WC1N 1AX, UK
[b] University of Greenwich, Chatham, Kent ME4 4TB, UK
[c] University College London, London WC1E 6BT, UK
[d] Spirogen Ltd, 29-39 Brunswick Square, London WC1N 1AX, UK

ARTICLE INFO

Article history:
Received 4 February 2011
Revised 11 April 2011
Accepted 12 April 2011
Available online 20 April 2011

Keywords:
Pyrrolobenzodiazepine (PBD)-conjugate
Inverted CCAAT box
Nuclear Factor Y
Topoisomerase IIα
Anticancer agents

ABSTRACT

A series of novel DNA-interactive C8-linked pyrrolobenzodiazepine (PBD)–heterocycle polyamide conjugates has been synthesised to explore structure/sequence-selectivity relationships. One conjugate (**2d**) has a greater selectivity and DNA binding affinity for inverted CCAAT sequences within the Topoisomerase IIα promoter than the known C8-*bis*-pyrrole PBD conjugate GWL-78 (**1b**).

The CCAAT box is a common DNA sequence motif present in direct or reverse orientation in the promoters of many eukaryotic genes. It is usually found approximately 80 base pairs upstream of the transcription start site and may be present in one or more copies. It provides a recognition site for a number of general transcription factors (known as CCAAT box binding proteins or factors) including the ubiquitously expressed Nuclear Factor Y (NF-Y), in which case protein-specific binding is necessary for CCAAT box activation.[1,2] Studies have shown that CCAAT box binding proteins such as NF-Y[3] are associated with a number of important cellular processes including cell cycle progression,[4] differentiation,[5] and cellular aging.[5,6] NF-Y has been shown to exert both stimulatory and inhibitory effects on gene expression, and an important link between NF-Y and p53 has emerged in which activation of p53 by DNA damage induces repression of G2/M genes through NF-Y association leading to cell cycle arrest. Conversely, P53 mutants commonly found in human tumour cells have an increased affinity for NF-Y, resulting in activation of growth-promoting genes under NF-Y control.[7,8] Therefore, targeting the interaction of NF-Y with DNA could be a potential strategy for blocking the proliferation of cancer cells.

There have been previous attempts to use small molecules to disrupt NF-Y/DNA binding both for experimental purposes and as a potential means to develop novel therapeutic agents.[9,10] We have previously reported the synthesis of a series of C8-linked PBD–poly(*N*-methylpyrrole) conjugates (**1a**–**f**, Fig. 1A), members of which have significant DNA recognition properties and the potential to modulate the activity of specific transcription factors.[11] These conjugates bind covalently through their C11-position to the C2-NH_2 functionality of guanine residues in the DNA minor groove with a preference for 5′-XGXW$_z$ motifs (X = any base, but mainly a purine; W = A or T; $z = 3 \pm 1$).[11] Hochhauser and co-workers demonstrated that one member of this family, GWL-78 (**1b**), can inhibit the binding of NF-Y to inverted CCAAT box sequences 1–3 (ICBs 1–3) within the human DNA Topoisomerase IIα (Topo-IIα) promoter.[12] **1b** was demonstrated to interact with a variety of CCAAT-containing promoters leading to p53-independent cell cycle arrest.[12]

In an effort to further investigate the interactions of **1b** with ICBs sites, and to improve on the potency and selectivity of the parent ligand, we prepared a library of six analogs of **1b** (**2a**–**f**, Fig. 1B) in which the pyrrole residues in the C8-polyamide chain were changed to various combinations of pyrrole (Py), imidazole (Im) or thiazole (Th) rings. These heterocycles were selected as they have been previously used by Dervan to enhance the sequence recognition of non-covalent minor-groove binding DNA-interactive ligands.[13] Thermal denaturation and DNA footprinting assays were employed to assess the DNA-binding affinity and sequence selectivity of these molecules, and their cytotoxicities were determined

* Corresponding author.
E-mail address: david.thurston@pharmacy.ac.uk (D.E. Thurston).

0960-894X/$ - see front matter © 2011 Elsevier Ltd. All rights reserved.
doi:10.1016/j.bmcl.2011.04.054

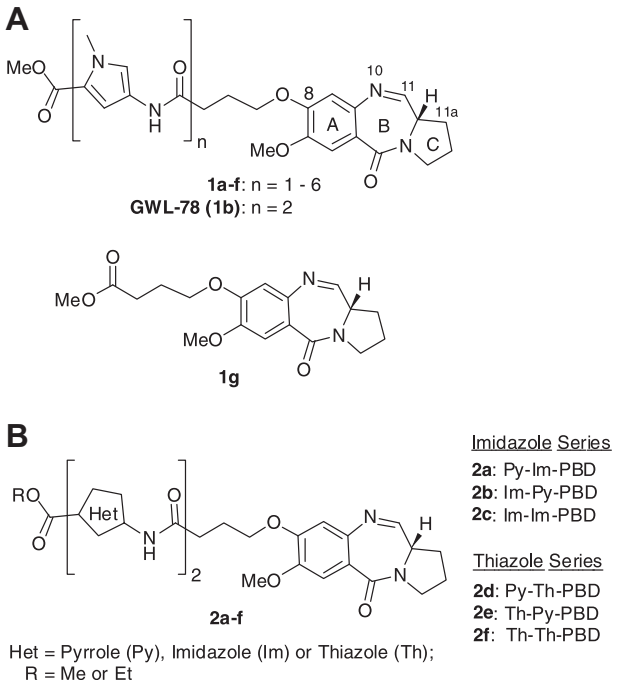

Figure 1. (**A**) Structures of the C8-linked pyrrolobenzodiazepine–poly(*N*-methylpyrrole) conjugates[11] including GWL-78 (**1b**), and the C8-coupled PBD-linker fragment **1g** upon which **1a–f** and **2a–f** are based. (**B**) The library (**2a–f**) of analogues of **1b** containing combinations of imidazole (Im), thiazole (Th) and pyrrole (Py) heterocycles in the C8-polyamide chain.

in the National Cancer Institute (NCI) 60-cell-line panel. The thiazole-containing conjugate **2d** emerged as superior to **1b** in terms of overall DNA-binding affinity, selectivity for specific ICB sequences and growth inhibitory potency.

The synthetic approach used to prepare PBD-conjugates **2a–f** is shown in Scheme 1. The heterocyclic amino esters **3a–c** and the Boc-protected heterocyclic amino acids **4a–c** were prepared according to literature methods[11,14] and then coupled together (using EDCI/DMAP) to produce the *N*-Boc-protected imidazole (**5a–c**) and thiazole (**5d–f**) dimers which, without purification, were deprotected to provide **6a–f**. These dimeric units were then coupled to the previously described[11] PBD capping unit **7** to obtain PBD conjugates **2a–f** in moderate to good yields.[15]

Table 1
Thermal denaturation and in vitro cytotoxicity data for the PBD–heterocyclic conjugates **2a–f**, **1b** (GWL-78) and the linker PBD **1g**.

Compound	ΔT_m[a] (°C)			Cytotoxicity (NCI 60-cell-line panel)[b]		
	0 h	4 h	18 h	GI_{50} (nM)	TGI (nM)	LC_{50} (μM)
2d	14.5	15.2	15.8	3.1	96.0	9.1
1b	13.7	14.5	15.1	11.0	120.0	10.0
2c	10.3	10.9	11.4	35.5	933.0	13.5
2b	10.0	10.7	11.2	100.0	1445.0	32.4
2e	9.3	9.6	10.2	14.8	363.0	19.1
2f	7.7	8.0	8.3	70.8	813.0	12.3
2a	2.8	3.0	3.1	691.8	4898.0	19.5
1g	0.2	0.3	0.4	1740.0	11,800.0	46.8

[a] Induced ΔT_m following incubation at 37 ± 0.1 °C for the time shown.[19] For control CT-DNA alone, ΔT_m = 67.82 ± 0.07 °C (mean from >90 experiments). All ΔT_m values are ±0.1–0.2 °C. For a fixed 1:10 molar ratio of [ligand]/[DNA], DNA concentration = 50 μM (base pairs) and ligand concentration = 5 μM, in aqueous sodium phosphate buffer [10 mM sodium phosphate + 1 mM EDTA, pH 7.00 ± 0.01].

[b] GI_{50}, TGI and LC_{50} values (the concentrations causing 50% growth inhibition, total growth inhibition, and 50% lethality, respectively) are mean across the 60-cell-line-panel.

Table 2
Minimum concentration of each PBD-conjugate required to provide a measurable footprint at the ICB1 and ICB2 sites

Compound	Identity	DNA footprinting potency[a] (μM)	
		ICB1	ICB2
2d	Py-Th-PBD	0.2	0.2
1b	Py-Py-PBD	1	1
2b	Im-Py-PBD	5	5
2c	Im-Im-PBD	25	5
2a	Py-Im-PBD	>25	>25
2e	Th-Py-PBD	>25	1
2f	Th-Th-PBD	>25	>25

[a] concentration (μM) at which DNA footprints were observed.

The relative overall binding affinities of **2a–f** were evaluated from their induced effects upon the melting behaviour (T_m) of double-stranded calf thymus (CT) DNA.[11,16–19] The results (Table 1) show that all the conjugated ligands increased the thermal stability of the DNA duplex but to different extents. In particular, the Py–Th–PBD conjugate (**2d**) had a higher DNA binding affinity than **1b** and all other library members, with a ΔT_m value of 14.5 °C without incubation (i.e., 0 h)[19] compared to 13.7 °C for **1b**. The Im-contain-

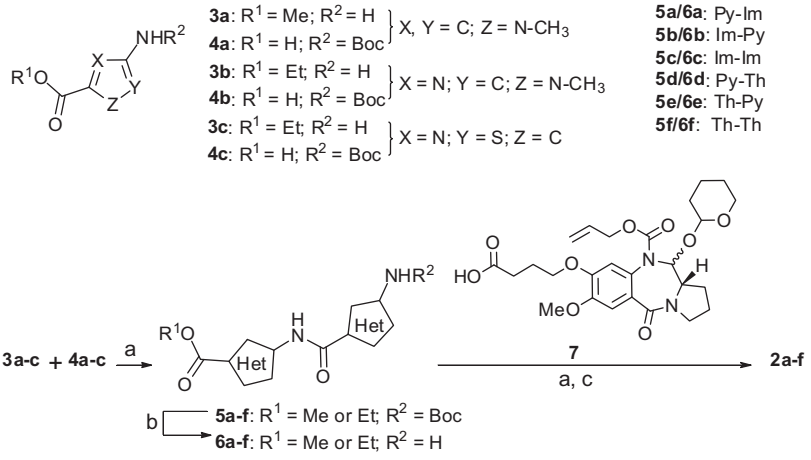

Scheme 1. Reagents and conditions: (a) EDCI, DMAP, CH_2Cl_2, 18–48 h, 35–99%; (b) CH_2Cl_2/TFA/H_2O (50:47.5:2.5 v/v), 30 min (or 4 M HCl in dioxane, 30 min, for the imidazole-containing dimers); (c) $Pd[PPh_3]_4$, pyrrolidine, CH_2Cl_2, 3 h, 30–55% (Het = generic heterocycle).

ing PBD conjugates **2b**–**c** and the Th-containing **2e**–**f** stabilised DNA less effectively than **2d** or **1b**, and the Im-containing **2a** had the lowest ΔT_m compared to all other compounds. For comparative purposes, the C8-coupled PBD-linker fragment **1g** (Fig. 1**A**) was evaluated in both the DNA thermal denaturation assay and in the NCI 60-cell-line panel (Table 1). It had only weak duplex DNA stabilizing properties (i.e., ΔT_m = 0.4 °C after 18 h) and was not appreciably cytotoxic compared to the PBD-conjugates **2a**–**f**, thus confirming the contribution of the C8-heterocyclic rings to the activity of **1b** and **2a**–**f**.

DNase I footprinting studies were carried out to evaluate the sequence selectivity of the PBD–polyamide conjugates using a new methodology described by Hartley and co-workers.[20] This involved the use of IR dyes rather than a radiolabel, with DNA fragments visualized on the gel through detection of the dyes with a diode laser. PBD conjugates **2a**–**f** and **1b** were footprinted against a 170 bp fragment of the human Topo-IIα promoter containing the ICB1 and ICB2 sites. All PBD–heterocycles were incubated with the DNA fragment at different concentrations (0 → 25 μM) overnight prior to DNase I cleavage. According to the literature,[11] incubating PBD C8-conjugates such as **1a**–**f** with DNA for 17 h should lead to complete covalent binding. The results are summarized in Table 2, and a typical gel resulting from the study is shown in Figure 2**A**.

The results demonstrate that substitution of an imidazole or thiazole unit for a pyrrole in the C8-polyamide chain of **1b** significantly affects the binding affinity and selectivity of the compounds for the CCAAT motifs. Conjugate **2d** showed the greatest binding affinity, generating measurable footprints at both ICB1 and ICB2 sites at 0.2 μM, a concentration 5-fold lower than for **1b** (1 μM) (Fig. 2**A**). In contrast, three imidazole- (**2a**–**c**) and two thiazole-containing (**2e**–**f**) PBD-conjugates had a lower affinity for the ICB sites. Interestingly, compounds **2c** and **2e** were able to discriminate between the two ICB sites, binding at a lower concentration to ICB2 (see Table 2).

The conjugates were also screened in the NCI 60-cell-line panel (Table 1). Once again, **2d** was found to be the most potent member of the series, with a greater cytotoxicity compared to **1b** and all other library members. Furthermore, it was found to be more active against breast, colon and renal cancer cells compared to other tumour types in the NCI panel. The mean GI_{50} value across all cell lines was approximately 3-fold lower than for **1b** (i.e., 3.1 vs 11.0 nM, respectively). These results correlate with the thermal denaturation and footprinting data, with **2d** exhibiting the highest potency in all assays. Furthermore, the GI_{50} value for **2d** (3.1 nM) is nearly 3000-times lower than its LC_{50} value (9.1 μM), consistent with its proposed mechanism of action as a transcription factor inhibitor.

Molecular modelling studies were performed in an effort to rationalize the superior DNA binding affinity and sequence selectivity of conjugate **2d** compared to **2a**, which had the lowest potency in all assays. In each case, a 5′-CTAC**G**ATTGGTTCTT-3′ duplex containing an ICB sequence (underlined) flanked by a 5′G (bold) as found in ICBs 1 and 2 in the Topo-IIα promoter was used. B-DNA was constructed with the AMBER package,[21] and the *xleap* program was used to make an initial graphical alignment of the ligand in the minor groove prior to forming a covalent attachment between the C11-position of the PBD and the C2-NH_2 of guanine-5 in the minor groove of the 15-mer DNA model. The PBD A-ring

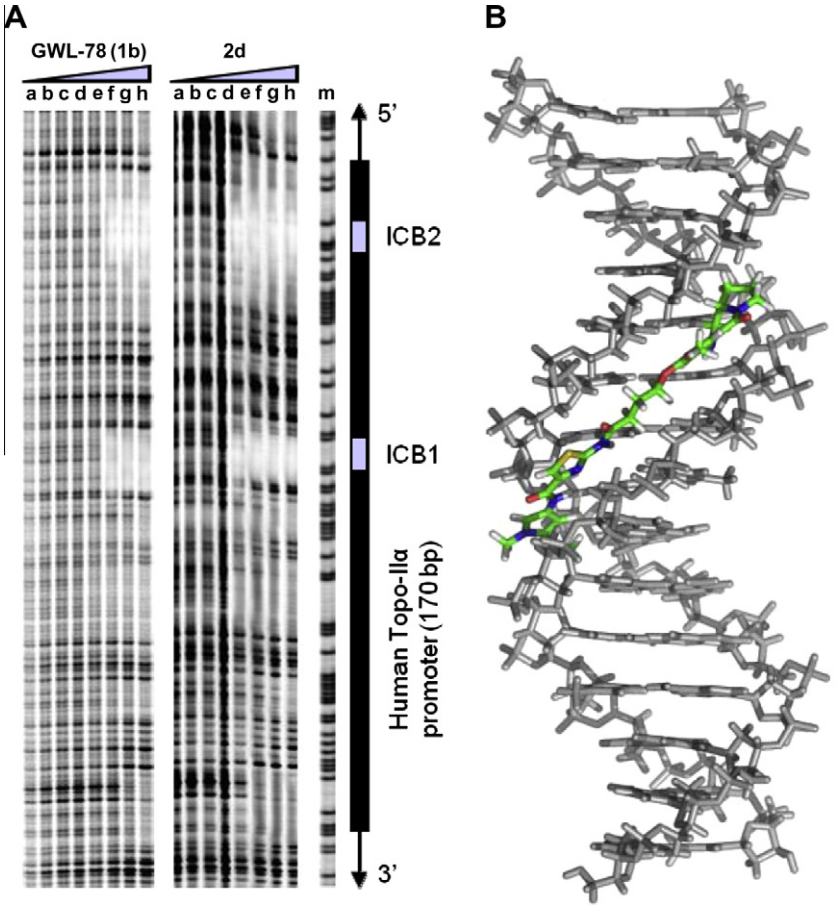

Figure 2. (A) DNase I footprinting gel showing the binding of PBD conjugates **1b** (GWL-78) and **2d** to a 170 bp fragment of the human Topo-IIα promoter. Footprints can be seen at both the ICB1 and ICB2 sequences as marked on the gel. Lanes a–h correspond to concentrations of 0, 0.0016, 0.008, 0.04, 0.2, 1, 5 and 25 μM, respectively. The marker lane (m) allowed sequence identification. (B) Model of complex of **2d** covalently bound to a 15-mer DNA duplex containing an embedded 5′-GATTGG-3′ tract.

was oriented towards the 3′-end of the covalently-modified strand with a *S*-configuration at the C11-position of the PBD, consistent with observations reported in the literature.[11] Subsequent minimization was performed using AMBER, initially applying a large positional restraint to the DNA only. This was gradually reduced to zero in further rounds of minimization. A long range non-bonded cut-off was applied along with use of the GBSA implicit solvent model and monovalent ion screening (0.2 M). After the energy minimization procedure, both bound conjugates appeared to be well-accommodated within the DNA minor groove with virtually no induced distortion of the overall host duplex structure. Figure 2**B** shows the excellent fit achieved by the most potent ligand **2d** in the minor groove of the ICB1 sequence when covalently bound to the C2-NH_2 of G5. Surprisingly, there were no obvious differences between the two models in terms of distortions or steric interactions that might account for the large difference in experimental binding affinities observed for **2a** and **2d**.

A further investigation centred on evaluating the free energy of binding by constructing the two ligands in their most appropriate conformations prior to covalent interaction. This was followed by graphical alignment in the minor groove by placing the N10 of each PBD moiety with its partial negative charge in close proximity to the partial positive charge of a C2-NH_2 hydrogen of guanine-5. A similar stepwise minimization procedure as used for the covalently-bound ligands was then applied, and free energy calculations undertaken using the AMBER MM-PBSA approach. This involved extracting 200 frames from a 2ns molecular dynamics simulation followed by calculation of the average free energy of binding in each case. However, this methodology also failed to provide an explanation for the observed difference in binding affinity between **2a** and **2d**. Perhaps this reflects the limitations of modeling approaches of this type to discriminate between ligands with relatively small structural differences when binding to a complex target such as DNA.

In summary, these results demonstrate that it is possible to modify the C8-*bis*-pyrrole side chain of GWL-78 (**1b**) to improve DNA binding affinity and selectivity for specific ICB sites within the human Topo-IIα promoter, although it is not yet possible to rationalize how the improved activity of **2d** relates to the structural change. Further studies of **2d** are underway to evaluate its ability to stabilize shorter fragments of DNA containing the ICB binding sequence, and to determine whether it can inhibit the binding of NF-Y to DNA in cells using methods such as chromatin immunoprecipitation (ChIP). In addition, the effect of extending the length of **2d** with further heterocycles is being investigated.

Acknowledgments

Dr. Emma Sharp is gratefully acknowledged for her help with preparing the manuscript. The authors thank EPSRC for a studentship for R.M.H. (Earmarked QUOTA Award 01300211), and Cancer Research UK for funding to D.E.T. (C180/A1060, SP1938/0402, SP1938/0201 and SP1938/0301) and J.A.H. (C2259/A9994).

References and notes

1. Mantovani, R. *Gene* **1999**, *239*, 15.
2. Higuchi, T.; Anzai, K.; Kobayashi, S. *Biochim. Biophys. Acta-Gen. Subj.* **2008**, *1780*, 274.
3. Ronchi, A.; Bellorini, M.; Mongelli, N.; Mantovani, R. *Nucleic Acids Res.* **1995**, *23*, 4565.
4. Sandri, M. I.; Isaacs, R. J.; Ongkeko, W. M.; Harris, A. L.; Hickson, I. D.; Broggini, M.; Vikhanskaya, F. *Nucleic Acids Res.* **1996**, *24*, 4464.
5. Marziali, G.; Perrotti, E.; Ilari, R.; Coccia, E. M.; Mantovani, R.; Testa, U.; Battistini, A. *Blood* **1999**, *93*, 519.
6. Matuoka, K.; Chen, K. Y. *Ageing Res. Rev.* **2002**, *1*, 639.
7. Di Agostino, S.; Strano, S.; Emiliozzi, V.; Zerbini, V.; Mottolese, M.; Sacchi, A.; Blandino, G.; Piaggio, G. *Cancer Cell* **2006**, *10*, 191.
8. Imbriano, C.; Gurtner, A.; Cocchiarella, F.; Di Agostino, S.; Basile, V.; Gostissa, M.; Dobbelstein, M.; Del Sal, G.; Piaggio, G.; Mantovani, R. *Mol. Cell. Biol.* **2005**, *25*, 3737.
9. Tolner, B.; Hartley, J. A.; Hochhauser, D. *Mol. Pharmacol.* **2001**, *59*, 699.
10. Mackay, H.; Brown, T.; Sexton, J. S.; Kotecha, M.; Nguyen, B.; Wilson, W. D.; Kluza, J.; Savic, B.; O'Hare, C.; Hochhauser, D.; Lee, M.; Hartley, J. A. *Bioorg. Med. Chem.* **2008**, *16*, 2093.
11. Wells, G.; Martin, C. R. H.; Howard, P. W.; Sands, Z. A.; Laughton, C. A.; Tiberghien, A.; Woo, C. K.; Masterson, L. A.; Stephenson, M. J.; Hartley, J. A.; Jenkins, T. C.; Shnyder, S. D.; Loadman, P. M.; Waring, M. J.; Thurston, D. E. *J. Med. Chem.* **2006**, *49*, 5442.
12. Kotecha, M.; Kluza, J.; Wells, G.; O'Hare, C. C.; Forni, C.; Mantovani, R.; Howard, P. W.; Morris, P.; Thurston, D. E.; Hartley, J. A.; Hochhauser, D. *Mol. Cancer Ther.* **2008**, *7*, 1319.
13. Dervan, P. B. *Bioorg. Med. Chem.* **2001**, *9*, 2215.
14. Boger, D. L.; Fink, B. E.; Hedrick, M. P. *J. Am. Chem. Soc.* **2000**, *122*, 6382.
15. *Data for* **2d**: A pale yellow solid (30% yield). ^{1}H NMR (acetone-d_6) (400 MHz): δ 11.29 (s, 1H, N–H), 9.28 (s, 1H, N-H), 7.81 (s, 1H, Th-H), 7.74 (d, 1H, J = 4.4 Hz, H-11), 7.53 (d, 1H, J = 1.9 Hz, Py-H), 7.40 (s, 1H, H-6), 6.96 (d, 1H, J = 2.0 Hz, Py-H), 6.81 (s, 1H, H-9), 4.19 (m, 2H, side chain H-1), 3.91 (s, 3H, O/N-CH_3), 3.87 (s, 3H, O/N–CH_3), 3.77 (s, 3H, O/N–CH_3), 3.69 (m, 1H, H-11a), 3.46 (m, 2H, H-3), 2.53 (s, 2H, side chain H-3), 2.36 (m, 2H, H-1), 2.26 (m, 2H, side chain H-2), 2.09 (s, 2H, H-2); LC–MS m/z (ES+): 595 ([M+H]$^+$); Acc. Mass $C_{28}H_{30}N_6O_7S$: calcd 595.1070, found 595.1957 ([M+H]$^+$).
16. McConnaughie, A. W.; Jenkins, T. C. *J. Med. Chem.* **1995**, *38*, 3488.
17. Bose, D. S.; Thompson, A. S.; Smellie, M.; Berardini, M. D.; Hartley, J. A.; Jenkins, T. C.; Neidle, S.; Thurston, D. E. *Chem. Commun.* **1992**, 1518.
18. Thurston, D. E.; Bose, D. S.; Howard, P. W.; Jenkins, T. C.; Leoni, A.; Baraldi, P. G.; Guiotto, A.; Cacciari, B.; Kelland, L. R.; Foloppe, M. P.; Rault, S. *J. Med. Chem.* **1999**, *42*, 1951.
19. The '0 h' values shown actually reflect ~30 min equilibration heating within the instrument used for the T_m assay. This is unavoidable and cannot be circumvented in temperature scan-based assays. Heating was applied at a rate of 1 °C/min in the 50–99 °C temperature range, with optical and temperature data sampling at 100 ms intervals. A separate experiment was carried out using buffer alone, and this baseline was subtracted from each DNA melting curve before data treatment. Experiments were conducted in triplicate.
20. Ellis, T.; Evans, D. A.; Martin, C. R. H.; Hartley, J. A. *Nucleic Acids Res.* **2007**, *35*. Article No.: e89.
21. Case, D. A.; Darden, T. A.; Cheatham III, T. E.; Simmerling, C. L.; Wang, J.; Duke, R. E.; Luo, R.; Merz, K. M.; Pearlman, D. A.; Crowley, M.; Walker, R. C.; Zhang, W.; Wang, B.; Hayik, S.; Roitberg, A.; Seabra, G.; Wong, K. F.; Paesani, F.; Wu, X.; Brozell, S.; Tsui, V.; Gohlke, H.; Yang, L.; Tan, C.; Mongan, J.; Hornak, V.; Cui, G.; Beroza, P.; Mathews, D. H.; Schafmeister, C.; Ross, W. S.; Kollman, P. A. University of California, San Francisco, 2006.